Applied Catalysis B: Environmental 227 (2018) 285–295

Contents lists available at ScienceDirect

Applied Catalysis B: Environmental

journal homepage: www.elsevier.com/locate/apcatb

Bacterial disinfection by the photo-Fenton process: Extracellular oxidation or intracellular photo-catalysis?

Stefanos Giannakis[a,*], Margaux Voumard[a,b], Sami Rtimi[a], Cesar Pulgarin[a,*]

[a] School of Basic Sciences (SB), Institute of Chemical Science and Engineering (ISIC), Group of Advanced Oxidation Processes (GPAO), École Polytechnique Fédérale de Lausanne (EPFL), Station 6, CH-1015 Lausanne, Switzerland

[b] School of Architecture, Civil and Environmental Engineering (ENAC), Environmental Engineering Institute (IIE), Laboratory for Water Quality and Treatment (LTQE), École Polytechnique Fédérale de Lausanne (EPFL), Station 2, CH-1015 Lausanne, Switzerland

ARTICLE INFO

Keywords:
Escherichia coli
Porin-deficient mutants
Photo-Fenton
Reactive oxygen species (ROS)
Intracellular oxidative stress

ABSTRACT

In this work, we evidence that despite the addition of the Fenton reagents in the bulk, the photo-Fenton mediated inactivation is mainly an intracellular process. We compare the inactivation kinetics of a typical *E. coli* strain that can exchange solutes with its environment through its outer membrane porins with its porinless mutant counterpart. The transport of Fe^{2+} and H_2O_2 into the bacterial cell was hypothesized to be the limiting factor of the photo-Fenton-mediated inactivation. This important pathway that could initiate intracellular oxidative chain reactions would be evidenced by the use of a porinless bacterial strain, derivative of MC4100 (TK821). The comparison among the typical *E. coli* K12 (ATCC 23716) and TK821 showed that the processes that constitute the photo-Fenton (solar, solar/Fe^{2+}, solar/H_2O_2) are greatly modified between the two strains. ATCC 23716 was always inactivated faster than the TK821, and a 45% and 150% difference in inactivation rate was measured for the solar/Fe^{2+} and the solar/H_2O_2 processes. The photo-Fenton process inactivation rates were doubled, and the contribution of the intracellular and extracellular pathways was estimated. The mechanisms taking place in the bulk were twice as important for TK821, while the inverse was estimated for the intracellular events in ATCC 23716. The results of this work demonstrate that porins are essentially a regulator of the photo-Fenton disinfection, and that is mainly an intracellular advanced oxidation process.

1. Introduction

The evolution of the Fenton process since its conception in 1894 [1] has witnessed tremendous leaps, from the single use as a decontamination process at acidic pH [2] to a possible water purification process aided by the sun, via discovery that it can still work at near-neutral pH with the aid of ferrioxalate [3] and the seminal publication of Rincon and Pulgarin that have succeeded in proving its function without complexing agents [4]. These findings have opened new pathways in (photo)Fenton research, and a renewed interest in a process that initially seemed impossible to apply. However, more than a decade later, the mechanistic studies have still to contribute in the disinfection process, since the bacterial inactivation is a complex process that deviates from the standard approach of chemical contaminant elimination at acidic pH, mostly because of the complex iron chemistry at neutral pH [5–7] and the variability of oxidants generated via the process, like the ferryl ion [8,9] and the hydroxyl radical [10,11].

In a previous paper, we have reviewed the action of the different constituents of photo-Fenton, and the importance they hold in synthesizing the combined process, against bacterial inactivation [12]. Briefly, the baseline solar process is causing inactivation of crucial oxidative stress protective enzymes [13] and the accumulation of these reactive oxygen species (ROS) leads to bacterial death [14]. Addition of H_2O_2 further imbalances the internal ROS [15], while Fe adds up also with a ligand-to-metal charge transfer-mediated mechanism of inactivation, due to cell wall damage and external ROS [16]. Nevertheless, the elucidation of the exact bacterial inactivation mechanism for the combined photo-Fenton process is still difficult to achieve, and most works limit to measuring specific aspects, such as contribution of external factors [17,18], or kinetic evaluation of disinfection [19].

The use of knock-out mutants [20–22] or modified microorganisms with fluorescent probes [23] is not a new practice in the process of identifying the mechanisms that govern bacterial inactivation. For instance, the biggest knowledge library on the internal oxidative mechanisms was performed with such strains [24,25]. Using catalase-deficient [26] or over-productive *E. coli* strains [27,28], the importance of this enzyme was established in controlling H_2O_2 stress and internal oxidative conditions. Also, the use of mutants explained other AOPs,

* Corresponding authors.
E-mail addresses: Stefanos.Giannakis@epfl.ch (S. Giannakis), Cesar.Pulgarin@epfl.ch (C. Pulgarin).

https://doi.org/10.1016/j.apcatb.2018.01.044
Received 9 November 2017; Received in revised form 17 January 2018; Accepted 19 January 2018
Available online 31 January 2018

such as TiO_2 photo-catalysis [29], or metal-based disinfection of cells [30]. Specifically, the strain used in the last study is deficient in porins, and its use has shown limited uptake of ions and a subsequent lower inactivation of cells. Porins are three classes of bacterial proteins that generate water channels in the outer membrane of the cell, and mediate the exchange of hydrophilic compounds to and from the external environment to the periplasm [31–33]. As it can be understood, their importance to maintaining bacterial homeostasis can be critical. Also, although initially thought that porins are mainly expressed in Gram-negative bacteria, findings indicate their presence in Gram-positive strains as well ([34] and references therein, and [35]), indicating the importance of this transport system in bacterial life cycle and in extension, in water or wastewater treatment.

In this work, we employ this porinless, modified *E. coli* strain, in an effort to control the influx of H_2O_2 and iron from the bulk towards the cells, and prove that the photo-Fenton process is an oxidative series of events taking place into the cell. The dark processes are firstly investigated as blank experiments of the combined photo-Fenton process. Afterwards, solar light alone, solar light in presence of low ppm amounts of Fe^{2+} or H_2O_2 and their simultaneous addition (photo-Fenton) were assayed. A variation of the aforementioned processes by addition of the Fenton reagents before solar exposure was also assessed. The difference in cultivability as well as the H_2O_2 and (dissolved) Fe profiles during dark and solar treatment processes are evaluated and the contribution of oxidants towards the extracellular or intracellular photo-Fenton processes are compared.

2. Materials and methods

2.1. Microbial methods

2.1.1. Typical E. coli (ATCC 23716) and mutant E. coli strain (TK821) preparation

The normal *E. coli* strain (i.e. wildtype K12) (ATCC 23716) was acquired from "Deutsche Sammlung von Mikroorganismen und Zellkulturen" (DSMZ, No. 498) and the mutant *E. coli* TK821 is a derivative of the MC4100 strain (DSMZ, No. 6574). The TK821 is the same as MC4100 but $ompF^-$ $ompC^-$ Tc^r; it involved the mutations of operons, which determine the expression of outer membrane proteins (Omp), such as OmpF and OmpC [36–39]. The wild strain of TK821 (MC4100) is isogenic with the K12 used in this study and thus they belong to the same phylogenetic lineage. This limits the differences that may happen due to the strain change. For both microorganisms, a colony was isolated from pre-cultures and was dispersed in 5 mL Luria-Bertani (LB) broth (10 g/L Bacto™ Tryptone, 5 g/L Yeast extract, and 10 g/L NaCl, in ultrapure water (Mili-Q). The bacterial growth was monitored by the optical density at 600 nm. The dispersion was incubated in the dark, under aerobic conditions and agitation. Their growth phase was monitored by the optical density at 600 nm (OD_{600}) until it reached exponential growth phase (0.8). 1% dilution into 250 mL fresh LB solution was then performed, and incubation took place until the stationary phase was reached (~15 h); SOD synthesis will then be normal, and KatE properly expressed by the RpoS system [40]. The bacterial suspension was centrifuged at 500 × *g* for 15 min, at 4 °C, and the supernatant was discarded and the remaining bacterial pellet was washed three times with saline solution (8 g/L NaCl and 0.8 g/L KCl). Finally, 25 mL of saline solution was added and the resulting bacterial suspension resulted in ~10^9 CFU/mL.

2.1.2. Sampling and enumeration of cells

The samples in the reactors were under constant stirring by magnetic bar (250 rpm) placed on magnetic stirrers. 1 mL of sample was recovered and stored in 1.5-ml sterile plastic Eppendorf vials for their transport from the reactors until their immediate enumeration (minute range). Bacterial count was performed by the standard plate count in 9-cm sterile petri dishes containing plate count agar (PCA, composition: 9.0 g/L agar, 1.0 g/L dextrose, 5.0 g/L tryptone, 2.5 g/L yeast extract in MQ water). 3–4 serial dilutions were performed to achieve measurable bacterial counts on the plates, and results are given in CFU/mL (average is presented, with < 20% standard deviation). All experiments were performed twice, in duplicates. Alternatively, when experiments are presented, the logarithmic units of bacterial cultivability reduction (logU) may be used for comparison reasons. The bacterial limit of detection was 10 CFU/mL (1 colony found in a dish where 0.1 mL of sample is plated). Fitting inactivation kinetics (Section 3.3) was done by Origin Pro 9.0 software for Windows, by linear regression.

2.2. Experimental procedure

2.2.1. Light source, reactors and experimental conditions

Solar light was provided by an Atlas Suntest CPS+ solar simulator, bearing a 1500-W Xenon lamp. The lamp emits 0.5% of the photons below 300 nm and 5–7% at the 320–400 nm region; UVC uncoated quartz glass cut-off filter was installed (290–800 nm emission). The apparatus allows a 560-cm^2 effective illumination surface and is constantly air-cooled. The maximum temperature reached 37′C during treatment. The irradiance was pre-set at 600 W/m^2, controlled by a global irradiance and UV radiometer couple (Models CM3 and CUV3, respectively, from Kipp & Zonen). The test took place in UVB-transparent pyrex glass reactors, containing 100 mL of 10^6 CFU/mL-spiked MQ water. All experiments took place in MQ water, at near-neutral starting pH (6.5). The final pH was no less than 5.8. The iron and H_2O_2 contents were chosen to be 1 and 10 ppm correspondingly, amounts that have been found to sufficiently exert the Fenton process in previous works ([16,41]). Practically, it does not represent water or wastewater treatment analogies, but a manner at which the bacterial kinetics can be easily followed by cultivability, while Fe/H_2O_2 measurements are above the LOQ for the respective methods. For the internal oxidative action experiments (Section 3.3) 5 ppm of the reagent (Fe or H_2O_2) was used, as Fe was deemed low to exert any effect on its own and H_2O_2 was sufficiently high and not oxidizing cells rapidly.

2.2.2. Iron and H_2O_2 measurements

For the colorimetric determination of extracellular (and in indirect manner, the intracellular) Fe and H_2O_2, a Shimadzu 1800 UV–vis spectrophotometer was used. Filtered and unfiltered samples (0.2 μm) were both assayed. The determination of iron concentration was performed by the Ferrozine method [42]. For each test, 1.6 mL of sample was mixed with 0.2 mL of 4.9 mM Ferrozine solution. Reduction of Fe^{3+} to Fe^{2+} was done by hydroxylamine (0.2 mL of a 10% w/w solution). Finally, measurement at 562 nm was performed. H_2O_2 concentration was determined by the addition of 10 μL of Titanium(IV) oxysulfate and subsequent measurement of the pertitanic acid at 410 nm. The Fe and H_2O_2 concentration was determined via pre-defined calibration curves. The limit of quantification for these methods are 0.3 μM with a 1 cm cell for iron [42] (Ferrozine method LOQ) and 0.1 mg/L LOQ for H_2O_2 spectrophotometric measurement.

2.3. Chemicals and reagents

All chemicals were used as received. Ferrous sulfate heptahydrate ($FeSO_4{\cdot}7H_2O$), Perdrogen™ (30% w/w) and Titanium (IV) Oxysulfate ($TiOSO_4$, 1.9–2.1%), plate count agar (PCA), Ferrozine (3-(2-Pyridyl)-5,6-diphenyl-1,2,4-triazine-*p,p′*-disulfonic acid monosodium salt hydrate) and Hydroxylamine Hydrochloride were purchased from Sigma-Aldrich (Switzerland).

2.4. Design of experimental plan

In principle, the experimental plan conceived to prove the importance of the porins in Fenton reagents' transport into the cell and the subsequent intracellular photo-Fenton process constituted in the step-

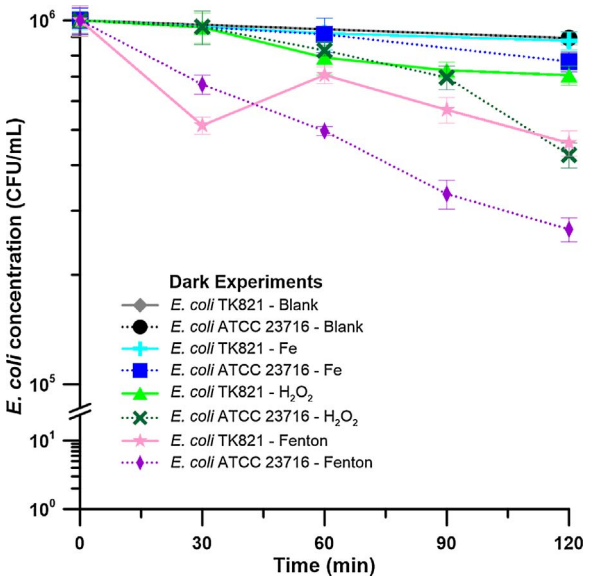

Fig. 1. *E. coli* inactivation in the dark: ATCC 23716 (dotted trace) vs TK821 (continuous trace).

wise construction of the photo-Fenton process, by its constituents. As such, the effect of Fe, H_2O_2 and both together (Fenton process) in absence of light are studied to assess the baseline damage. Afterwards, starting by light exposure, the addition of Fe, H_2O_2 and both reagents was introduced and studied. Finally, in order to assess the possibility that the transport process might require time to have quantifiable difference among the two strains, the action of Fe was compared when inserted at the beginning of illumination time or 30 min before, and H_2O_2 and Fe + H_2O_2 were tested 30 and 60 min before illumination, under the rationale that H_2O_2 is stabler than Fe at neutral pH and the effect could be visible after 30 min; Fe precipitation might mask the corresponding 60-min test.

3. Results and discussion

3.1. Dark (control) experiments and solar-based tests

Experiments in absence of light that define the boundary conditions of the experiments to follow were conducted and the results are summarized in Fig. 1. The cultivability of the typical *E. coli* K12 (here on: ATCC 23716) and TK821 in the dark was followed in absence of Fenton reagents, with Fe (1 ppm), with H_2O_2 (10 ppm), and both reagents (dark Fenton process). Of primary importance was to ensure that the two strains behave similarly in absence of stresses in the dark; the hypothesis was confirmed and further dark control tests ensued; a summary of the results is given at the Supplementary Table S1.

In general, the dark processes tested here did not alter bacterial cultivability significantly, hence, here we will mostly focus on the prevalent mechanism. More specifically, Mili-Q water has low effect in bacterial viability in the 2-h experimental duration; any effects might be due to the die-off of sensitive cells attributed to the osmotic shock. Fe barely had any effect on the viability of any of the two strains. The baseline process when iron was added into the bulk in the form of Fe^{2+}, was the transport inside the periplasm takes place via the non-specific porins of the outer membrane [43,44], followed by the transport into the cytoplasm by various systems [45], as recently reviewed [44]. After the natural process of iron oxidation by dissolved O_2 (from Fe^{2+} to Fe^{3+}), the transport changes and is facilitated by different systems, such as siderophoric proteins [46], which gather iron from precipitates or the external environment, and require specific receptors to pass to the periplasm [47]. Hence, the two strains will present different behavior as long as Fe^{2+} exists in the bulk in high amounts, and any cultivability loss was due to Fe transport into the cell and temporary disruption of Fe balance [48] or aggregation caused after the oxidation of Fe^{2+} to Fe^{3+}, which is an excellent coagulant agent [49].

Concerning hydrogen peroxide addition, porins have been found to regulate its diffusion [31,50]. Its diffusion is possible through lipids under cell osmotic stress conditions and the comparable physical properties with H_2O can allow its passage [33,51]. Afterwards, H_2O_2 that normally enters the cytoplasm is scavenged primarily by alkyl hydroperoxide reductase (ahpCF), and most probably KatG [40], as it is expressed under H_2O_2 stress, regulated by the OxyR system, contributes in high amounts (> μM) of H_2O_2, in a process that is much faster than the influx rate [52,53]. Due to the limited diffusion in the mutant strain, we can observe that the cultivability was slightly higher (on the verge of statistical significance, with Pearson correlation test = 0.88, P-value = 0.044), probably to the H_2O_2 flux into the normal *E. coli* cell and reaction with Fe, to produce HO· and damage the microorganism.

The simultaneous presence of both Fe and H_2O_2 had a more notable effect, but still correlated, i.e. not significant (Pearson value 0.82, but $P > 0.05$ so not validated in the 95% confidence interval). The first difference among the strains was observed; lower counts have been measured in ATCC 23716 concentration, as Fe and H_2O_2 can be transported into the cell and enhance the internal Haber-Weiss reactions. Initially, ferric iron into the cell is reduced to ferrous and the Fenton process then ensues (Eq. (1)–(3)).

$$Fe^{3+} + O_2^{\circ -} \rightarrow Fe^{2+} + O_2 \quad (1)$$

$$Fe^{2+} + H_2O_2 \rightarrow Fe^{3+} + HO^- + HO^\circ \quad (2)$$

$$O_2^{\circ -} + H_2O_2 \rightarrow HO^- + HO^\circ + O_2 \quad (3)$$

Furthermore, the production of hydroxyl radicals due to the Fenton process is similar (k_2 = 63–70 $M^{-1} s^{-1}$), and the inactivation rate caused by this action, is not affected by the porins. The process is limited by the kinetics of regeneration of Fe^{3+} to Fe^{2+} in the bulk (see Eq. (4)) below [54]:

$$Fe^{3+} + H_2O_2 \rightarrow Fe^{2+} + HO_2^\circ + H^+ \quad k_3 = 0.01 M^{-1}s^{-1} \quad (4)$$

Nevertheless, the maximum inactivation reached was 0.57 and 0.35 logU inactivation for the ATCC 23716 and TK821 strains, respectively, and it shows that the effect of the dark processes was limited (note the scale in Y axis). The baseline process is almost negligible (below 0.8, the values of the Pearson test indicate low correlation) and hence, can be left out of consideration for the subsequent steps.

After the characterization of the dark blank experiments and the explanation of the biological significance of porins, the solar processes are presented. Fig. 2(a–d) describes the solar-based tests (irradiance: 600 W/m^2), namely solar light alone, solar light/Fe^{2+} (1 ppm), solar light/H_2O_2 (10 ppm) and solar light/Fe/H_2O_2 (photo-Fenton, 1/10 ppm), typical concentrations for near-neutral photo-Fenton in drinking water [55]. Solar light (Fig. 2a) is the baseline process for the next to follow and is important to note possible deviations among the typical and mutant strains. The solar-induced inactivation followed the typical inactivation curve, with prolonged delay phase [56,57] due to the low irradiance [58]. The variation in cultivability among the two strains is negligible and lies within the margin of experimental error, hence, there was no difference between the two strains, during this phase of experiments. The solar disinfection process has been suggested to be an internal oxidative one [12]. Apart from the mutations caused by the direct action of UVB light mostly [59], since UVA has limited absorbance by the genetic material, there exist indirect intracellular pathways initiated by UVB and UVA light. The most prominent ones leading to bacterial inactivation involve antioxidant enzyme inactivation, like the catalases and the peroxidases [25], followed by accumulation of short and long-living Reactive Oxygen Species (ROS) such as $^1O_2$, $O_2^{\circ -}$ and H_2O_2 [24]. These ROS can react with different

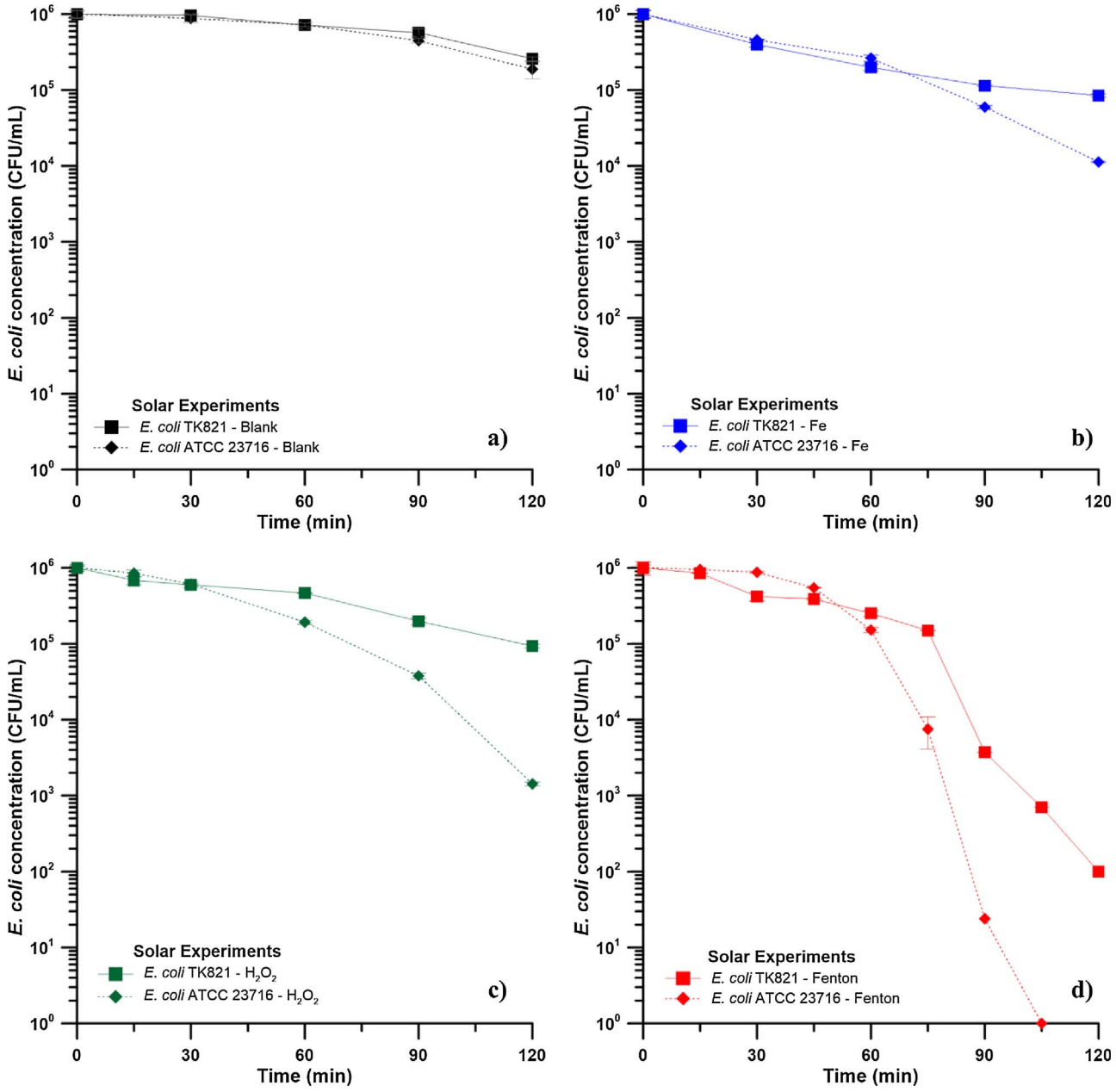

Fig. 2. *E. coli* ATCC 23716 (dotted trace) vs TK821 (continuous trace) inactivation in solar-assisted processes. A) Solar light alone. B) Solar light with 1 ppm Fe^{2+}. C) Solar light with 10 ppm H_2O_2. D) Solar photo-Fenton process, with 1 ppm Fe^{2+} and 10 ppm.

components, like the reaction of $^1O_2$ with DNA [60], as well as the iron-bearing compounds of the cell. For instance, $O_2^{\circ -}$ was found to reduce thymine bases, or by reaction with H_2O_2 to produce HO· [61], and to reduce metals from the [4Fe-4S] clusters; this will release ferrous iron in the bulk [62] and with the H_2O_2 left unregulated, it will result in further HO· production and cause the enhancement of the internal Fenton process by intracellular iron and the accumulated oxidants [63,64].

Addition of iron in the bulk (Fig. 2b) inflicts two important changes in the inactivation process, according to the iron localization, i.e. iron that is transported in the cell or that stays in the bulk. As mentioned before, the porins can facilitate the passage of ferrous in the cell, and enhance the intracellular Fenton process taking place after catalases deactivation (possibly both KatE and KatG) [40] and H_2O_2 accumulation. The most common forms of Fe in water are the following [2,65] (Eq. (5)–(9)):

$$[Fe(H_2O)_6]^{3+} + H_2O \leftrightarrow [Fe(OH)(H_2O)_5]^{2+} + H_3O^+ \quad (5)$$

$$[Fe(OH)(H_2O)_5]^{2+} + H_2O \leftrightarrow [Fe(OH)_2(H_2O)_4] + H_3O^+ \quad (6)$$

$$2[Fe(OH)(H_2O)_5]^{2+} \leftrightarrow [Fe_2(OH)_2(H_2O)_8]^{4+} + 2H_2O \quad (7)$$

$$[Fe_2(OH)_2(H_2O)_8]^{4+} + H_2O \leftrightarrow [Fe_2(OH)_3(H_2O)_7]^{3+} + H_3O^+ \quad (8)$$

$$[Fe_2(OH)_3(H_2O)_7]^{3+} + [Fe(OH)(H_2O)_5]^{2+} \leftrightarrow [Fe_3(OH)_4(H_2O)_5]^{5+} + 7H_2O \quad (9)$$

Upon estimation, the octahedral iron^{2+}-water molecule structure has a diameter of < 6 Å [66–68]. If we consider that the diameter of the bacterial porins is 10–11 Å [69,70], the iron transport via this channel is very likely. Consequently, iron will pass to the cytoplasm e.g. by periplasmic siderophoric proteins [47]; seven bacterial transport systems are postulated to exist [71], and will facilitate the passage. After transport, iron normally is regulated by specific proteins [72] and will be deposited in ferritins, after its oxidation to Fe^{3+} [73]. Upon light

irradiation, and the modification of the normal iron storage functions of the cell, the ferrous iron has more opportunities to react with the intracellular ROS explained before, leading to high intracellular inactivation events. That explains the inactivation profile seen in Fig. 2b: The inactivation pattern showed slightly faster cultivability loss for the porinless TK821 compared with the typical *E. coli* strain, tendency that was inverted after 60 min. This trend indicates higher initial external inactivation, followed by enhanced internal one. If in ATCC 23716 iron is transported inside the cell, then the initial inactivation due to the external events is lower, combined with maintaining of antioxidant enzyme activity, hence the higher cultivable cells for 1 h. Afterwards, TK821 continue to get inactivated in similar or lower rate, but for ATCC 23716 the process is changed, and we suggest that it aggravates internally, since the external conditions are the same, with high accumulation of oxidants and iron into the cell. Part of this effect is that Fe^{3+} from the oxidation of Fe^{2+} in the bulk is transported by different mechanisms than Fe^{2+}, which have not been deliberately modified in the mutant strain, and therefore should be similar. Besides, the iron that has not been transported into the cell can form complexes with extracellular structures. This complexation with carboxylic groups of the siderophoric compounds, such as the transferrins [44] or other negatively charged compounds [74,75], can facilitate a ligand to metal charge transfer; iron is oxidized and the sacrificial donor gets damaged by reduction (Eq. (10)). Another possibility is iron aqua complexes that absorb light perform the same process with water as a Lewis base and subsequently produce HO· [76] (e.g. Eq. (11)):

$$[Fe^{+3} - L]^{3+} + 2H_2O \xrightarrow{hv(LMCT)} [Fe(H_2O)_2]^{2+} + L^{\circ +} \quad (10)$$

$$[Fe^{3+}(OH)(H_2O)_5]^{2+} + H_2O \xrightarrow{hv(LMCT)} [Fe^{2+}(H_2O)_6]^{2+} + HO^{\circ} \quad (11)$$

Addition of H_2O_2 (Fig. 2c) enhanced inactivation compared to solar light alone. TK821 presented 0.5 log further inactivation, reaching 1 log after 2 h of solar exposure. However, ATCC 23716 presented a 3-log enhancement of cultivability loss, after a 30-min lag. Similarly to Fe, we can consider the intracellular and extracellular H_2O_2 actions separately. H_2O_2 that diffuses into the cell will enhance the internal photo-Fenton process, especially Eq. (2), with the subsequent HO· generation being lethal to the cell. Comparing the size of H_2O_2 molecule (1.2–1.4 Å [31,76,77]) and the bacterial porins (10–11 Å), we can safely suggest that it can diffuse, even more easily that iron did. The addition of H_2O_2, depending on the amount can initiate two different types of inactivation, namely Mode I and II. For Mode I, the added H_2O_2 was proven to induce modification in catabolic and biosynthetic functions, help release loose iron from the iron/sulfur clusters and to generate HO·, or by electron transfer directly, without the mediation of Fe [20,62,78]. This would explain the different inactivation profiles between the two different strains, with steady inactivation rate for the mutant compared to the enhanced inactivation demonstrated in the normal *E. coli*, due to the shift in peroxidase and catalase activity. The Mode II of H_2O_2 inactivation concerns the extracellular events, with H_2O_2 reacting with the cellular membrane and increasing its permeability, allowing the influx of more H_2O_2 into the cell [79,80]. This is made possible by oxidation of cell wall components; H_2O_2 has a mild oxidative activity (here 0.815) and is higher than the membrane oxidation potential. We should not exclude also that, H_2O_2 which stays outside the cell will undergo (limited) homolysis and generate HO· [81], adding up to the extracellular inactivation of bacteria. However, as the concentration among the two strains might differ due to different diffusion, this damage will become less in normal *E. coli* compared to the mutant strain.

Finally, adding both Fenton reagents under solar light (Fig. 2d) induces notable inactivation in both strains. Nevertheless, different patterns were noted. TK821 again presented a higher initial loss of cultivability, but less profound inactivation compared to ATCC 23716, which, after 60 min, demonstrated 2–3 logU higher inactivation. A summary of the events that take place suggests that the simultaneous addition of Fe and H_2O_2 causes a massive oxidative wave of HO· in the bulk, which damages cells externally. Under light, the Fe^{3+} can subsequently reduce to Fe^{2+} either with ligand to metal charge transfer (LMCT) by the cell wall, the aqua complexes and/or the H_2O_2 reductive action. The photo-Fenton process can thus be sustainable for a longer period at near-neutral pH. In parallel, we have to consider that the mechanisms of iron transport will remain as explained before (at least the passive ones), as well as the H_2O_2 transport inside the cell. Upon diffusion the photo-Fenton cycle will be significantly higher than the cases presented before; evidence from a different microorganism than *E. coli* has shown that the process is mainly an intracellular one [41]. This internal catalytic cycle is sustained by the regeneration of Fe^{3+} back to Fe^{2+} by the mechanisms mentioned earlier, and the use of components (such as the DNA backbone [82] and the siderophoric proteins) as ligands for the regeneration of Fe^{3+} to Fe^{2+} and the Fenton reaction facilitation. There is however, a difference among the two microorganisms at the first stages of the process. This pattern that was once more repeated, and leads is to consider that the inactivation is indeed a function of the intracellular events, by enhancement of the internal photo-Fenton process due to the transport via the bacterial porins. The inactivation of TK821 became profound after a prolonged lag, which can be attributed to the delayed cell wall lysis as inactivation mechanism, while for ATCC 23716, the internal and external stress present synergy. Finally, we have to mention here that the process is in constant competition with iron precipitation to Fe-hydroxides. Although it is initiated as a homogeneous Fenton, it quickly gets transformed to homogeneous/heterogeneous, led by dissolved iron, iron complexed to the cell and siderophores, or regenerated via LMCT, and the ferric hydroxides, respectively. The presence of the aforementioned components (sideophores, cell wall and components, light) give rise to constant Fe^{2+} generation, effective photo-Fenton process, and thus the difference among the two strains; Fe^{3+} is regulated in a similar manner.

3.2. Dark incubation experiments followed by solar light

In all experiments with the Fenton reagents presented before, a delay of 30–60 min was observed. Questions such as the time of diffusion of the oxidants and the effects of H_2O_2 penetration, as well as Fe precipitation are still open. Hence, a new set of experiments was performed, with addition of each reagent 30 or 60 min prior to illumination. The results are summarized in Fig. 3.

Fig. 3a presents the different response of ATCC 23716 and TK821, if Fe^{2+} is added at t = 0 or 30 prior to illumination. Compared to addition at t = 0, adding Fe^{2+} 30 min prior to illumination presented different inactivation kinetics for both ATCC 23716 and TK821. Although the improvement in TK821 kinetics is 1 logU over the 2-h experiment, and remained quasi-constant throughout the experiment, ATCC 23716 at t = 60 and 120 min presented a 2- and 4-logU decrease in cultivability, respectively. In the normal test (addition of Fe^{2+} at t = 0), the initiation of light probably coincides with the deactivation of the ferrous and ferric iron transport activity of the cells. Most probably, the abundance of iron in the environment activates further assimilation by the bacterial mechanisms, and higher intracellular Fe-related events. When iron is added earlier, there is a high soluble fraction due to the siderophoric activity, which brings iron into the cell, while allowing better formation of Fe^{3+} complexes for the external fraction of iron. If we also take into consideration the similar rates of TK821 inactivation regardless of the time addition of iron, these events indirectly evidence the transport into the cell and the enhancement of the oxidative events that take place (by the ATCC 23716 kinetics), as well as the enhanced LMCT with the bacterial cell wall (by the TK821 kinetics).

Fig. 3b presents the 30- and 60-min prior addition of H_2O_2 before illumination. In overall, there was up to 50% decrease in the time necessary to inactivate all cells, for both ATCC 23716 and TK821. More specifically, ATCC 23716 inactivation increased with increased incubation time, while for TK821 there was no increase beyond 30 min

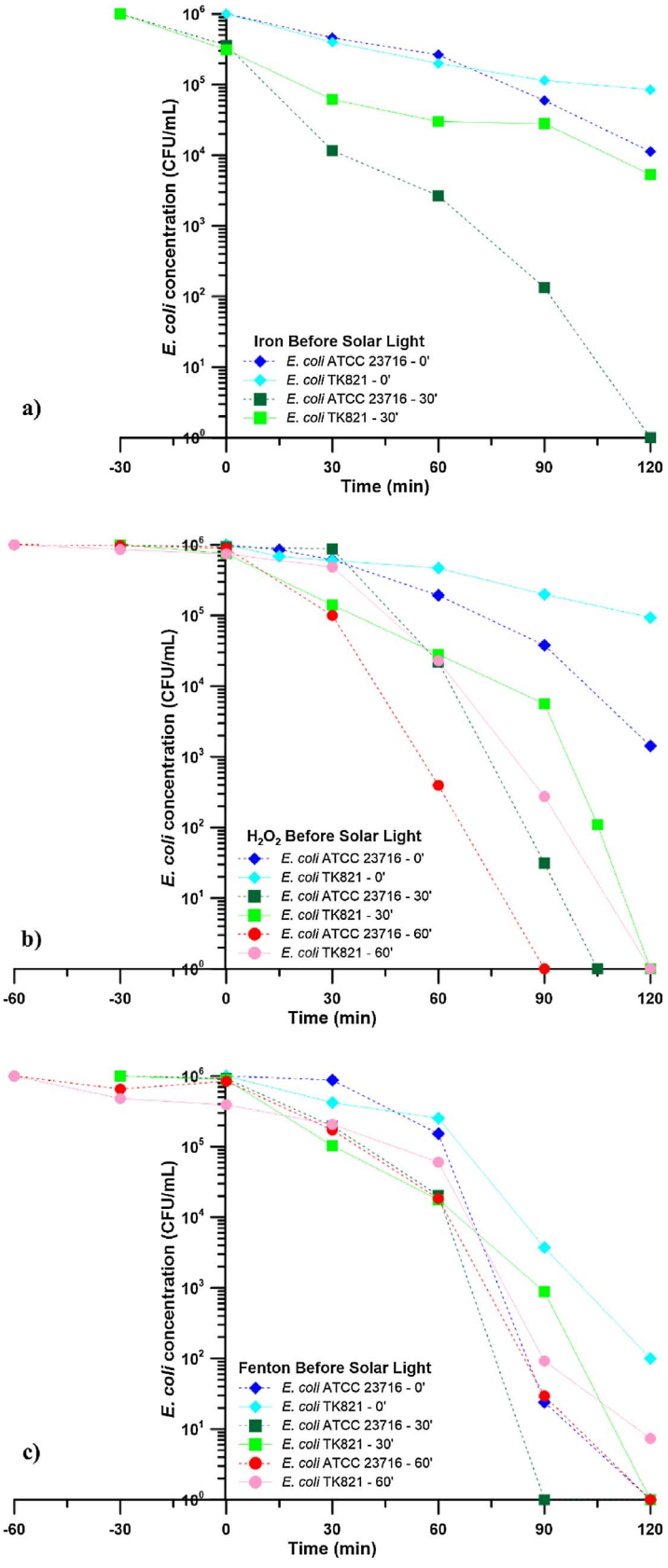

Fig. 3. *E. coli* ATCC 23716 (dotted trace) vs TK821 (continuous trace) inactivation in solar-assisted processes, with prior addition of Fe, H_2O_2. A) Solar light with 1 ppm Fe^{2+}, at t = −30 and t = 0 min. B) Solar light with 10 ppm H_2O_2, at t = −60, −30 and t = 0 min c) Solar photo-Fenton process, with 1 ppm Fe^{2+} and 10 ppm H_2O_2, at t = -60, −30 and t = 0 min.

incubation. Once again, at exposure of t = 30 min, the difference among the two strains started to appear, but after 60 or 90 min, the difference became important (> 2 logU). Adding H_2O_2 before the illumination allows two mechanisms to take place: i) diffusion of H_2O_2 into the cell, which gets fast scavenged only in μM amounts, and not in our tests (see Fig. 1), but has not great difference among 30 and 60 min of prior addition and ii) the oxidation of the cell membrane. The external action, the gradient of H_2O_2 concentration in the periplasmic space and

the H_2O_2 that are present inside, once light is provided to the system they fuel an efficient photo-Fenton process for the normal *E. coli*; the mutant strain and the ATCC 23716 suffer from the same extracellular damages. Most probably, in overall, the observed kinetics is an indication of the higher external damage via direct oxidation by H_2O_2 in TK821, compared to ATCC 23716, as well as the importance of H_2O_2 transport into the cell.

Finally, Fig. 3c indicated the differences if cells were exposed to the Fenton process prior to illumination. While 30 min (and less for 60 min) of dark incubation inflicted notable difference in ATCC 23716, further prior addition did not significantly enhance TK821 inactivation. At 30 min of exposure prior to irradiation, there is an important (3 logU) difference among the strains after 60–90 min of solar exposure; this deviation is not as high if cells were incubated for 60 min, most probably due to the decrease in oxidants' concentration. During the dark incubation period, the ongoing Fenton process inactivates both types of cells, and the iron oxidation advances in similar manner. The only difference lies in the influx of oxidants in ATCC 23716, which reflects in the inactivation kinetics. Nevertheless, since generally the TK821 inactivation was considerably slower than the ATCC 23716 respective one, this brings further proof to the concept of decrease of transport via bacterial porins. It is becoming obvious, that the porinless bacteria, that blocked the Fe^{2+} transport, as well as the H_2O_2 influx, after the light was provided to the system they suffered less profound damages than the normal *E. coli*: that is the result of the activity and the contribution of the porins in regulation of external substances.

3.3. Fenton's reagents transport into the cell is the key to internal photo-inactivation

In this part, in order to evidence and quantify the difference in inactivation kinetics between the two strains, we compare the inactivation rates presented in the two distinct experimental parts; the results are summarized in Fig. 4. In principle, the inactivation rate of ATCC 23716 and TK821 can be adequately modeled (mostly $R^2 > 90\%$) by first order kinetics, seen at Fig. 4a. As observed in Fig. 3a, for solar light the rates do not differ significantly (< 25%). However, addition of any of the two Fenton reactants enhances bacterial cultivability loss, depicted in 45% and 150% higher rates for solar/Fe and solar/H_2O_2 processes. The difference among the two could be firstly attributed to the difference in size and difficulty in transport into the cell, as well as the post-transport fate; at neutral pH iron will not remain soluble for long, hence the lower activity, while H_2O_2 can react even with the non-soluble forms of iron (heterogeneous photo-Fenton). Hence H_2O_2 is more important reagent in bacterial inactivation. Finally, the simultaneous addition of both reagents enhances solar inactivation and ATCC 23716 present 60% faster inactivation rates compared to the TK821.

If we consider the components of the photo-Fenton process (solar light, Fenton reaction) and the localization of the damage (intracellular, extracellular), then from the rates measured we can distinguish the contribution of each process. The generated ROS activity, both intracellular and extracellular can be approximated by subtracting the solar inactivation from the photo-Fenton process. The difference is a compelling 65% higher for ATCC 23716, due to the total ROS activity, inside or outside the cell, if we assume that the Fenton reagents all result in ROS generation. However, if from this process we subtract the combined solar/Fe and solar/H_2O_2 process, and the proposition of internal transport of H_2O_2 and Fe, then the external ROS contribution is 96% higher in TK821. This is supported by the difference observed in Fig. 2b–d. Finally, if the difference between the total and the external ROS is taken, then we get an 89% higher intracellular contribution in ATCC 23716. We suggest that this difference in inactivation rates distribution around the process leaves no doubts on the action and localization of the damages during the photo-Fenton process.

Beyond this point, for the second experimental set, we measured the kinetics before and after the illumination period, for the addition of Fe or H_2O_2, separately. In order to better compare the two processes, we considered the reaction between oxidants and bacteria at molecular level. For 100 mL reactors, the differences in H_2O_2 or iron concentrations (5 ppm initial addition, Supplementary Fig. S1) measured in molecules of Fe or H_2O_2, and the removal of cells per second was considered; the amount of H_2O_2 or Fe for the elimination of 1 cell per second is now compared. The results are summarized in Fig. 4b.

For the Fe^{2+} experiments, in the dark we note logarithmic difference in the amount of molecules necessary to inactivate 1 cell/sec, evidencing the difference explained initially. This difference remains equally high when light is provided to the system, quantifying the synergy between solar light and Fe. When H_2O_2 was inserted in the dark, similar rates are observed for both ATCC 23716 and TK821. This comes as no surprise, since i) the H_2O_2 that gets transported into the cells is converted to H_2O and O_2 by catalase (KatG) and peroxidase (ahpCF) activity [40] and ii) the only inactivation damage is due to cell wall oxidation, providing with this result. However, when light is given to the system, the molecules necessary to inactivate 1 cell/sec is considerably lower for ATCC 23716, since light affects the catalase functions. Less molecules are necessary, since there is no intracellular defense and the oxidative processes lead to cell inactivation. In TK821, similar rates are observed, since H_2O_2 is not transported inside the cell and the killing takes place mostly externally, as explained before. This trend was confirmed in higher concentrations of Fe and H_2O_2 (25 ppm), that showed similar profiles of Fe and H_2O_2 (data not shown) and call for further experimentation on the specific modes of action for both Fe and H_2O_2, intracellular Fe and H_2O_2 measurements, as well as the combined (photo-Fenton) process.

3.4. Integrated bacterial inactivation mechanism

According to the experimental findings and the comparison of the biological and kinetic evaluation with the relevant literature, we hereby present the inactivation mechanism, taking into account the specific role of the porins in the bacterial inactivation. Fig. 5(a–d) summarizes the inactivation mechanisms in absence/presence of light and Fenton reagents. For simplicity the various pathways have been numbered in each panel (top and bottom parts show ATCC 23716 and TK821, respectively), and pathways analyzed in one panel will not be repeated if not necessary.

In absence of light and Fenton reagents, both strains shown in Fig. 5a, top and bottom panel for ATCC 23716 and TK821 behave similarly, and their homeostasis mechanisms follow. 1) Bacteria have the enzymatic mechanisms to control the endogenic production of ROS, as by-products of their respiration process, such as KatG catalase (CAT), alkyl hydroperoxide reductase (AhP), and superoxide dismutase (SOD). 2) The protein storage and transport is controlled by the (iron regulating) *Fur* gene and achieved by the action of siderophoric proteins (SID).

When the Fenton reagents are added into the system (Fig. 5b), the difference among the two strains lies in the function of the porins. 1) In ATCC 23716, H_2O_2 diffuses into the cytoplasm, where the enzymes responsible for regulation are scavenging the influx for some time (apparently not completely, so it dies later); ahpCF alkyl hydroperoxide reductase and KatG catalase is expressed under H_2O_2 stress. In TK821 this pathway is blocked by the lack of porins. 2) Fe^{2+} passes to the cytoplasm via the porins and the corresponding transport systems, where is stored in relevant structures. Similarly to H_2O_2, this pathway is blocked in TK821. 3) Fe^{3+} generated through Fe^{2+} oxidation via O_2 or H_2O_2 is transported via different mechanisms into the cell, where is also stored. The modifications of TK821 still permit Fe^{3+} transport into the cell. 4) The excess of both reagents initiates an intracellular Fenton reaction, with HO· production and oxidative damages into the cell. 5) In TK821 the Fenton process is slower due to the Fe^{3+} initial iron form. 6) The simultaneous presence of Fe and H_2O_2 in the bulk leads to the HO· production via the Fenton process, which inactivates both

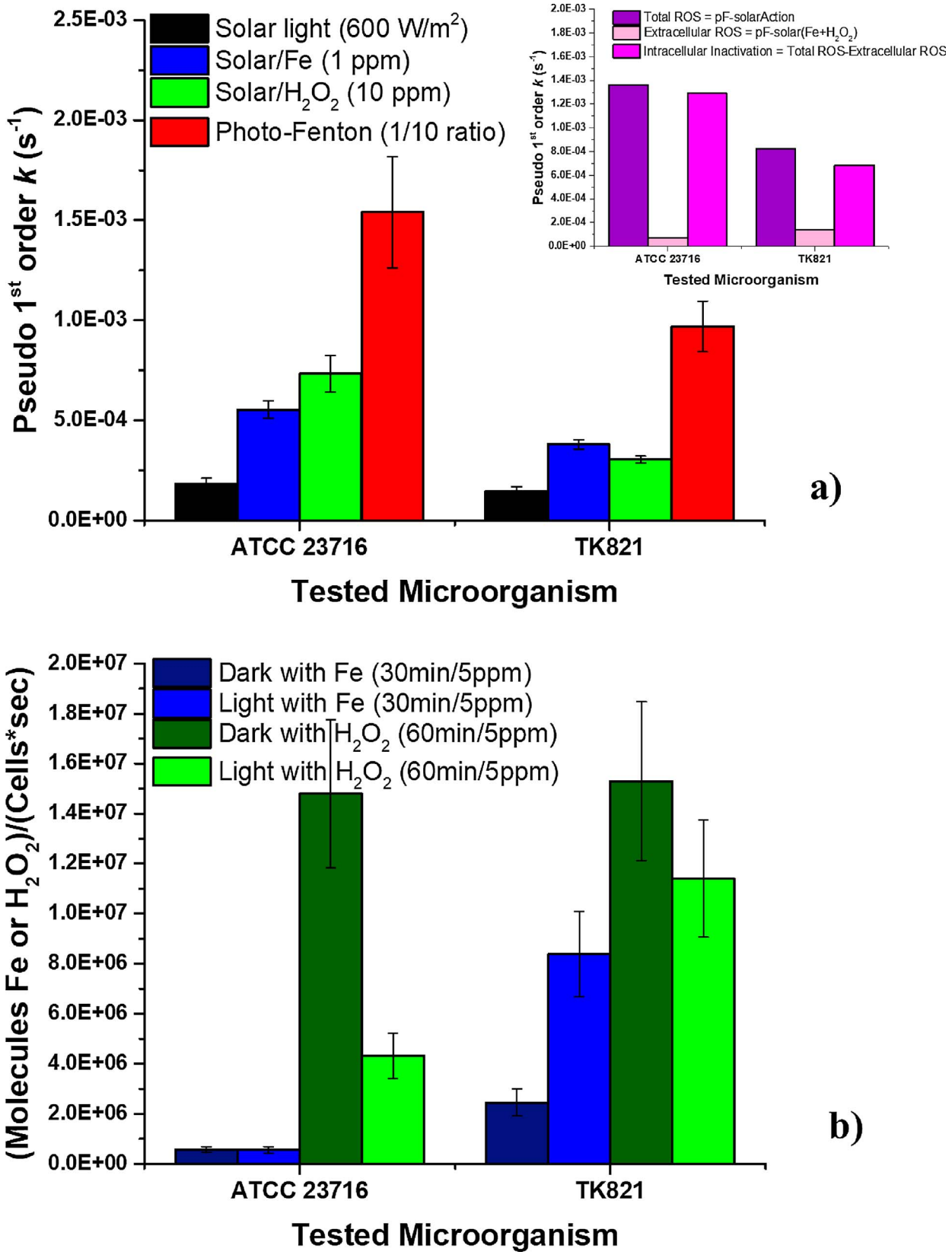

Fig. 4. Kinetic evaluation of *E. coli* inactivation for ATCC 23716 and TK821. A) Apparent 1st order kinetic constant. Inset: Total, intracellular and extracellular ROS-mediated inactivation rates. B) Oxidants necessary to inactivate 1 cell per sec.

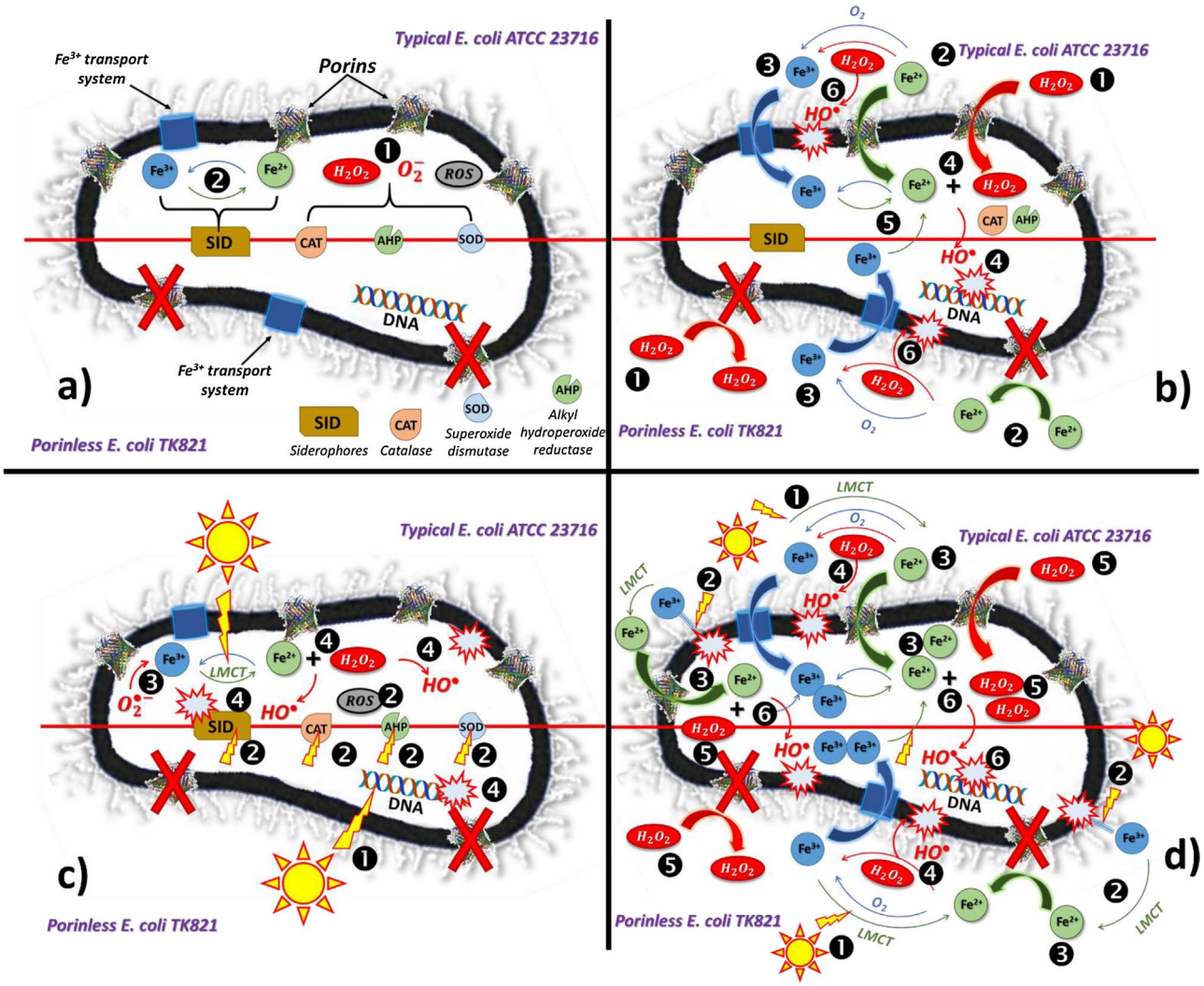

Fig. 5. Summary of the intracellular and extracellular inactivation mechanisms and the differences among typical K12 and porinless *E. coli*. In all panels (a–d), the top part shows the mechanisms involved in ATCC 23716 and the bottom the ones in TK821, separated by a red line; the intracellular mechanisms are similar. A) Normal state of *E. coli* in the dark; common for both strains. B) Changes inflicted by the addition of Fe^{2+} and/or H_2O_2, without irradiation. C) Inactivation of *E. coli* by solar light; common for both strains. D) Changes inflicted by addition of Fe^{2+} and/or H_2O_2 in irradiated samples. (For interpretation of the references to colour in this figure legend, the reader is referred to the web version of this article.)

bacterial strains due to the extracellular membrane damages.

Addition of light to the system, without the presence of the Fenton reagents (Fig. 5c) initiates a new series of internal events, since the effect on the membrane is negligible. Since the inactivation of the two strains is similar, the pathways presented are true for both ATCC 23716 and TK821. 1) In principle, UVB and UVA in a lesser extent, damage the DNA via the formation of thymine dimers. 2) More importantly, light affects the main activity of the ROS-scavenging and iron bearing proteins, and excess H_2O_2 and other ROS are generated inside the bacteria. 3) The ROS generated by the malfunction of enzymes will affect the iron bearing structures and lead to the release of iron in the cell. 4) The presence of ROS and their action against iron structures initiates the release of Fe and its reaction with H_2O_2, ensuing the production of HO· via an intracellular Fenton reaction. The HO· non-selectively oxidize intracellular structures within diffusion length, including DNA, cytoplasmic proteins and cell wall components.

In the last step, when the Fenton reagents are added in the bulk (Fig. 5d), the corresponding photo-Fenton process is more than the simple addition of the previous actions, as new pathways are initiated that aggravate the damage outside, and more importantly, inside the cell. 1) Oxidation of Fe^{2+} to Fe^{3+} is partially recovered by the LMCT process with Fe^{3+} using water as a Lewis base and the simultaneous production of HO·. 2) Another LMCT pathway is suggested between the bacterial cell wall and Fe^{3+}; the reaction leads to reduction of Fe^{3+} to Fe^{2+} and the oxidation of the sacrificial ligand (cell wall). These two pathways are common for both strains. 3) Fe^{2+} that is added in the bulk will get transported inside the ATCC 23716 cell, and cause imbalance, compared to the absence of this pathway in TK821. 4) Fe^{2+} will get oxidized to Fe^{3+} with H_2O_2 (producing HO·) or with O_2, and the Fe^{3+} could still get transported into the cell (in both strains). 5) The external addition of H_2O_2, will accumulate into the cell in normal *E. coli*, but in lesser extent in TK821; the KatG and ahpCF protective action is no longer present. The action of light affects both strains, in pathways 4 and 5, as the transport of Fe^{3+} into the cell and its fate not certain, and the H_2O_2/ROS accumulation will be lower in TK821, since there is low diffusion into the cell. 6) The over-accumulation of iron, in combination with the ROS will initiate internal oxidative events in both strains, but more importantly, in the typical *E. coli* that have higher intracellular H_2O_2 and Fe amounts.

4. Conclusions

In this work, an important part of the action of the near-neutral photo-Fenton process was found to be controlled by the bacterial porins. The major finding of this study is that the porinless (TK821) present considerably lower inactivation rates, compared to their

homologous ATCC 23716 ones. The cells have similar life cycles and although solar light inactivation was comparable, addition of Fe^{2+} and H_2O_2 was significantly modified due to the presence/absence of bacterial porins.

The localization of the damage was thereby assessed with important differences among the two strains. The normal *E. coli* were fast inactivated due to the transport of Fe^{2+} and H_2O_2 into the malfunctioning cell, due to the action of the solar light. However, porinless bacteria are suggested to be damaged mainly externally, in presence of solar light and the addition of the Fenton reagents.

Modifying the of Fe and H_2O_2 addition time into the bulk (dark incubation prior to exposure to light), was proven to modify the kinetics, in a manner that supports our initial hypothesis. Transport of Fe^{2+} (and Fe^{3+}) and H_2O_2 into the cell has been found to affect kinetics, always resulting in higher inactivation for both strains. In all cases, ATCC 23716 presented faster inactivation compared to TK821 and the initial higher losses of TK821 are suggested to be a result of the higher extracellular Fenton process taking place due to lower reagents' transport into the cell. No improvement was found by prolonging the dark incubation periods with the Fenton reagents, as ATCC 23716 scavenge the oxidants and start the experiments with lower amounts and ATCC suffer some external damages but the limiting step of the Fenton reaction does not allow high inactivation.

Finally, as estimated by the reaction rate constants, the photo-Fenton process was found to be essentially an intracellular process, since the external ROS action and internal inactivation rates were found to be more significant for porinless and normal *E. coli*, respectively. The necessary amount of Fenton reagents needed to inactivate cells, verified the inactivation kinetics' findings, and almost a double increase in the demand is noted for the TK821. This holds important insights in the current view of the photo-Fenton disinfection process, as it contributes to the understanding of bacterial inactivation pathways. The practical implications that could derive directly from this work, would be the recommendation of prior incubation of WW in H_2O_2 before iron addition and exposure to solar light, as it has been found to reduce residence times of treatment in our system.

Acknowledgements

Stefanos Giannakis and Cesar Pulgarin would like to acknowledge the European project WATERSPOUTT H2020-Water-5c-2015 (GA 688928) for the financial support. We also thank the anonymous reviewers for their constructive comments and insights that improved the overall quality of the manuscript.

Appendix A. Supplementary data

Supplementary data associated with this article can be found, in the online version, at https://doi.org/10.1016/j.apcatb.2018.01.044.

References

[1] H. Fenton, J. Chem. Soc. Trans. 65 (1894) 899–910.
[2] E. Neyens, J. Baeyens, J. Hazard. Mater. 98 (2003) 33–50.
[3] M. Cho, H. Chung, W. Choi, J. Yoon, Appl. Environ. Microbiol. 71 (2005) 270–275.
[4] A.-G. Rincón, C. Pulgarin, Appl. Catal. B: Environ. 63 (2006) 222–231.
[5] L. Emmenegger, R. Schönenberger, L. Sigg, B. Sulzberger, Limnol. Oceanogr. 46 (2001) 49–61.
[6] J.P. Jolivet, C. Chanéac, E. Tronc, Chem. Commun. 10 (2004) 481–487.
[7] J.F. Barona, D.F. Morales, L.F. González-Bahamón, C. Pulgarín, L.N. Benítez, Appl. Catal. B: Environ. 165 (2015) 620–627.
[8] W.C. Bray, M. Gorin, J. Am. Chem. Soc. 54 (1932) 2124–2125.
[9] J.Y. Kim, C. Lee, D.L. Sedlak, J. Yoon, K.L. Nelson, Water Res. 44 (2010) 2647–2653.
[10] R.G. Zepp, B.C. Faust, J. Hoigne, Environ. Sci. Technol. 26 (1992) 313.
[11] J.J. Pignatello, E. Oliveros, A. MacKay, Crit. Rev. Environ. Sci. Technol. 36 (2006) 1–84.
[12] S. Giannakis, M.I. Polo López, D. Spuhler, J.A. Sánchez Pérez, P. Fernández Ibáñez, C. Pulgarin, Appl. Catal. B: Environ. 199 (2016) 199–223.
[13] S. Mishra, J. Imlay, Arch. Biochem. Biophys. 525 (2012) 145–160.
[14] S. Giannakis, Environ. Sci. Pollut. Res. (2017) 1–17, http://dx.doi.org/10.1007/s11356-017-0926-x First Online: 19 December 2017.
[15] D. Spuhler, J.A. Rengifo-Herrera, C. Pulgarin, Appl. Catal. B: Environ. 96 (2010) 126–141.
[16] C. Ruales-Lonfat, N. Benítez, A. Sienkiewicz, C. Pulgarín, Appl. Catal. B: Environ. 160 (2014) 286–297.
[17] E. Ortega-Gomez, P. Fernandez-Ibanez, M.M. Ballesteros Martin, M.I. Polo-Lopez, B. Esteban Garcia, J.A. Sanchez Perez, Water Res. 46 (2012) 6154–6162.
[18] E. Ortega-Gómez, M.B. Martín, B.E. García, J.S. Pérez, P.F. Ibáñez, Appl. Catal. B: Environ. 148 (2014) 484–489.
[19] J. Rodríguez-Chueca, M.P. Ormad, R. Mosteo, J.L. Ovelleiro, Chem. Eng. Sci. 138 (2015) 730–740.
[20] K. Keyer, J.A. Imlay, Proc. Natl. Acad. Sci. 93 (1996) 13635–13640.
[21] J.A. Imlay, S.M. Chin, S. Linn, Science 240 (1988) 640–642.
[22] T. An, H. Sun, G. Li, H. Zhao, P.K. Wong, Appl. Catal. B: Environ. 188 (2016) 360–366.
[23] M. Castro-Alférez, M.I. Polo-López, P. Fernández-Ibáñez, Sci. Rep. 6 (2016) 38145.
[24] J.A. Imlay, Annu. Rev. Microbiol. 57 (2003) 395–418.
[25] J.A. Imlay, Annu. Rev. Biochem. 77 (2008) 755–776.
[26] J.A. Imlay, S. Linn, J. Bacteriol. 169 (1987) 2967–2976.
[27] M.K.S. Ballo, S. Rtimi, S. Mancini, J. Kiwi, C. Pulgarin, J.M. Entenza, A. Bizzini, Appl. Microbiol. Biotechnol. 100 (2016) 5945–5953.
[28] S. Mancini, J.A. Imlay, Mol. Microbiol. 96 (2015) 744–763.
[29] G. Gogniat, S. Dukan, Appl. Environ. Microbiol. 73 (2007) 7740–7743.
[30] S. Rtimi, V. Nadtochenko, I. Khmel, J. Kiwi, Chem. Commun. 53 (2017) 9093–9096.
[31] D. Aguayo, N. Pacheco, E.H. Morales, B. Collao, R. Luraschi, C. Cabezas, P. Calderón, F. González-Nilo, F. Gil, I.L. Calderón, Arch. Biochem. Biophys. 568 (2015) 38–45.
[32] H. Nikaido, Mol. Microbiol. 6 (1992) 435–442.
[33] G.P. Bienert, J.K. Schjoerring, T.P. Jahn, Biochim. Biophys. Acta (BBA) – Biomembr. 1758 (2006) 994–1003.
[34] M. Besnard, B. Martinac, A. Ghazi, J. Biol. Chem. 272 (1997) 992–995.
[35] W. Achouak, T. Heulin, J.-M. Pagès, FEMS Microbiol. Lett. 199 (2001) 1–7.
[36] X.-Z. Li, H. Nikaido, K.E. Williams, J. Bacteriol. 179 (1997) 6127–6132.
[37] I. Martínez-Flores, R. Cano, V.H. Bustamante, E. Calva, J. Puente, J. Bacteriol. 181 (1999) 556–562.
[38] A.P. Pugsley, C.A. Schnaitman, J. Bacteriol. 133 (1978) 1181–1189.
[39] P. Prohinar, S.A. Forst, D. Reed, I. Mandic-Mulec, J. Weiss, Mol. Microbiol. 43 (2002) 1493–1504.
[40] J.A. Imlay, Nat. Rev. Microbiol. 11 (2013) 443.
[41] S. Giannakis, C. Ruales-Lonfat, S. Rtimi, S. Thabet, P. Cotton, C. Pulgarin, Appl. Catal. B: Environ. 185 (2016) 150–162.
[42] E. Viollier, P.W. Inglett, K. Hunter, A.N. Roychoudhury, P. Van Cappellen, Appl. Geochem. 15 (2000) 785–790.
[43] G. Porcheron, A. Garénaux, J. Proulx, M. Sabri, C.M. Dozois, Front. Cell. Infect. Microbiol. 3 (2013).
[44] C.K. Lau, K.D. Krewulak, H.J. Vogel, FEMS Microbiol. Rev. 40 (2015) 273–298.
[45] R. Ge, X. Sun, Biometals 25 (2012) 247–258.
[46] H. Boukhalfa, A.L. Crumbliss, Biometals 15 (2002) 325–339.
[47] K.D. Krewulak, H.J. Vogel, Biochim. Biophys. Acta (BBA)-Biomembr. 1778 (2008) 1781–1804.
[48] V. Braun, K. Hantke, W. Koester, Met. Ions Biol. Syst. 35 (1998) 67–146.
[49] J. Rodríguez-Chueca, M. Morales, R. Mosteo, M. Ormad, J. Ovelleiro, Photochem. Photobiol. Sci. 12 (2013) 864–871.
[50] I.L. Calderón, E. Morales, N.J. Caro, C.A. Chahúan, B. Collao, F. Gil, J.M. Villarreal, F. Ipinza, G.C. Mora, C.P. Saavedra, Res. Microbiol. 162 (2011) 214–222.
[51] G.P. Bienert, A.L. Møller, K.A. Kristiansen, A. Schulz, I.M. Møller, J.K. Schjoerring, T.P. Jahn, J. Biol. Chem. 282 (2007) 1183–1192.
[52] L.C. Seaver, J.A. Imlay, J. Bacteriol. 183 (2001) 7173–7181.
[53] L.C. Seaver, J.A. Imlay, J. Bacteriol. 183 (2001) 7182–7189.
[54] J. De Laat, H. Gallard, Environ. Sci. Technol. 33 (1999) 2726–2732.
[55] S. Giannakis, M.I. Polo López, D. Spuhler, J.A. Sánchez Pérez, P. Fernández Ibáñez, C. Pulgarin, Appl. Catal. B: Environ. 198 (2016) 431–446.
[56] M. Berney, H.U. Weilenmann, A. Simonetti, T. Egli, J. Appl. Microbiol. 101 (2006) 828–836.
[57] S. Giannakis, A.I. Merino Gamo, E. Darakas, A. Escalas-Cañellas, C. Pulgarin, Chem. Eng. J. 253 (2014) 366–376.
[58] S. Giannakis, E. Darakas, A. Escalas-Cañellas, C. Pulgarin, Chem. Eng. J. 281 (2015) 588–598.
[59] R. Bensasson, E. Land, T. Truscott, Excited States and Free Radicals in Biology and Medicine: Contributions from Flash Photolysis and Pulse Radiolysis, (1993) (Tokyo).
[60] J.-L. Ravanat, T. Douki, J. Cadet, J. Photochem. Photobiol. B 63 (2001) 88–102.
[61] J.D. Hoerter, A.A. Arnold, D.A. Kuczynska, A. Shibuya, C.S. Ward, M.G. Sauer, A. Gizachew, T.M. Hotchkiss, T.J. Fleming, S. Johnson, J. Photochem. Photobiol. B 81 (2005) 171–180.
[62] S. Jang, J.A. Imlay, J. Biol. Chem. 282 (2007) 929–937.
[63] J. Hoerter, A. Pierce, C. Troupe, J. Epperson, A. Eisenstark, Photochem. Photobiol. 64 (1996) 537–541.
[64] J.A. Imlay, Curr. Opin. Microbiol. 24 (2015) 124–131.
[65] S.H. Lin, C.C. Lo, Water Res. 31 (1997) 2050–2056.
[66] L.M. Brines, M.K. Coggins, P.C.Y. Poon, S. Toledo, W. Kaminsky, M.L. Kirk, J.A. Kovacs, J. Am. Chem. Soc. 137 (2015) 2253–2264.
[67] L. Skogareva, G. Shilov, A. Karelin, J. Struct. Chem. 53 (2012) 907–914.
[68] P. Gütlich, H.A. Goodwin, Spin Crossover in Transition Metal Compounds I, Springer Science & Business Media, 2004.

[69] K. Simpson, N. Bevan, P. Hastwell, P. Eidam, P. Shah, E. Gogo, S. Rees, A. Brown, J. Biomol. Screen. 18 (2013) 441–452.
[70] H. Nikaido, J. Biol. Chem. 269 (1994) 3905–3908.
[71] V. Braun, Int. J. Med. Microbiol. 291 (2001) 67–79.
[72] D. Touati, Arch. Biochem. Biophys. 373 (2000) 1–6.
[73] B. Halliwell, J. Gutteridge, Biochem. J. 219 (1984) 1.
[74] X. Châtellier, D. Fortin, G.G. Leppard, F.G. Ferris, Eur. J. Mineral. 13 (2001) 705–714.
[75] X. Châtellier, M.M. West, J. Rose, D. Fortin, G.G. Leppard, F.G. Ferris, Geomicrobiol. J. 21 (2004) 99–112.
[76] P.A. Gigure, O. Bain, J. Phys. Chem. 56 (1952) 340–342.
[77] S. Abrahams, R. Collin, W. Lipscomb, Acta Crystallogr. 4 (1951) 15–20.
[78] S. Park, X. You, J.A. Imlay, Proc. Natl. Acad. Sci. U. S. A. 102 (2005) 9317–9322.
[79] B. Halliwell, O.I. Aruoma, FEBS Lett. 281 (1991) 9–19.
[80] J.A. Imlay, S. Linn, J. Bacteriol. 166 (1986) 519–527.
[81] A. Eisenstark, R. Buzard, P. Hartman, Photochem. Photobiol. 44 (1986) 603–606.
[82] J.A. Imlay, S. Linn, Science 240 (1988) 1302–1309.